

Gravitational waves from slow combustion of a neutron star to quark star

Shailendra Singh

Indian Institute of Science Education and Research Bhopal, Bhopal, India

shailendra17@iiserb.ac.in

and

Ritam Mallick

Indian Institute of Science Education and Research Bhopal, Bhopal, India

mallick@iiserb.ac.in

and

R Prasad

Indian Institute of Science Education and Research Bhopal, Bhopal, India

rprasad@iiserb.ac.in

ABSTRACT

Fluctuation at the neutron star center gives rise to a small deconfined quark core very close to the star center. The density discontinuity at the quark-hadron boundary initiates a shock wave, which propagates outwards of the star. The shock is strong enough to combust nuclear matter to 2-flavor quark matter in the star. The 2-flavor quark matter is not stable and there is an excess of down quarks. The 2-flavor matter settles to a stable 3-flavor matter in the weakly interacting time-scale. In this paper particularly study the conversion of 2-flavor matter to 3-flavor matter is carried out. We set up a differential equation for the conversion of the excess of down quarks to strange quarks involving weak reaction and diffusion of quarks. Calculating the reaction rate we solve the differential equation to find the velocity of the conversion front. The conversion velocity is about 0.002 times of the speed of light and the time taken for the conversion is about 1.96 millisecond. Once the front velocity is known we find the change in density profile of the star. As the conversion front moves out of the star the density profile changes bringing about a change in the quadrupole moment of the star. The change in the quadrupole moment is reflected in the GW amplitude which is of the order of $10^{-24} - 10^{-23}$. The power spectrum has a peak frequencies of around 10–20 kHz. Such amplitude and peak frequency is a unique signature of shock-induced first-order phase transition.

Subject headings: dense matter, equation of state, shock waves

1. Introduction

The theory of strongly interacting particles, known as Quantum chromodynamics, predicts that at high temperature and/or density the fundamental degree of freedom are not hadrons but quarks and gluons. Therefore, at high enough density/temperature there is deconfinement transition from hadrons to quarks and gluons. Earth based experiments with heavy ion collision in LHC, RHIC colliders probes the state of matter at high temperature and non-vanishing small chemical potential and found the state of quark gluon plasma (QGP). Theoretical studies with lattice simulation at zero chemical potential states that a smooth crossover transition happens from hadrons to QGP at high temperature. However, there is no ab-initio calculation for matter at finite chemical potential due to the infamous sign problem in lattice calculations. Phenomenological QCD model exists for finite baryon densities whose predictions matches quite well till nuclear saturation densities (Kruger et al. 2013). However, the phase transition (PT) at finite chemical potential happens at much higher densities. Therefore, the nature of PT at such densities, a strong first order or smooth crossover, is still unclear. One of the naturally occurring laboratories for testing matter properties at high densities are the interior of neutron stars (NSs). Recent, simultaneous detection of gravitational waves and electromagnetic signals from binary neutron star mergers has given hope that we can probe the interior of NS with better precision and thus improve the understanding of the matter properties occurring at high densities.

The merger GW170817 of binary NS has four phases (Abbott et al. 2017), the inspiral, merger and the postmerger and finally the ringdown. The signal detected from GW170817 was from the inspiral phase, from where we calculate the tidal deformability of the inspiral stars and thereby an estimate of their masses and spins (Faber & Rasio 2012; Baiotti & Rezzolla 2017). The merger is still beyond the scope of LIGO where one expects the density and temperature to increase and thereby the chances of phase transition from NM to QM. If such a phase transition happens during this time then they would leave their footprints during the merging and postmerger phases (Hinderer et al. 2008; Read et al. 2009; Pozzo et al. 2013; Agathos et al. 2015; Chatzioannou et al. 2018).

Recently there has been much work on what would be the footprint of such a PT happening in NS and how the merger and postmerger signal would change if there is a PT. Most et al (Most et al. 2018) did a binary merger simulation and found that there would be a phase difference in the evolution of the GW signal during the postmerger phase if the hypermassive NS has quarks in them. However, there is still ambiguity whether such signals would be unambiguous signals of PT. Recent studies have also explored the fact that the post merger GW frequency of stars which has undergone a PT would be very different from the normal postmerger frequency (Most et al. 2018). The empirical relationship between postmerger frequency and tidal deformability deviates significantly for hypermassive stars which has undergone PT during merging (Bauswein et al. 2019). Therefore, the holy grail of such signals remains in the merging and the postmerger phase which is still beyond the capability of present detectors. However, upcoming projects and detectors are trying to improve their detection capability significantly.

Most of the signals studied in the literature discusses signatures which comes after the PT has taken place and from the difference in EoS of NM and QM. However, the actual process of PT is not captured as it is assumed to happen instantaneously. However, if it is a shock induced PT then the actual process of PT can leave signals which can be detected with GW detectors. The shock induced PT has been studied previously in great detail by several authors (Bhattacharyya et al. 2006; Drago et al. 2007; Mishustin et al. 2015; Prasad & Mallick 2018, 2019; Mallick & Irfan 2019). Primarily they discusses that a sudden density fluctuation in the star induces an shock wave at the star core. This shock is strong enough to combust NM to QM and as the shock wave propagates out it mimics and PT in the star. The PT is assumed to be a two step process, the first step converts NM to defonfined 2-flavor QM in the strongly interacting time-scale and the second step converts unstable 2-flavor QM to stable 3-flavor QM in the weak time-scale (Bhattacharyya et al. 2006; Olinto 1991; Niebergal et al. 2010). In this article we would study how the 2-flavor matter converts to 3-flavor matter and how the GW is emitted from the star during this conversion. We will give a template of the GW signals which can originate from such a PT. The results qualitatively should be robust and would not depend strongly on the choice of EoS as long as PT can happen and 3-flavor matter is stable than NM at such densities.

The paper is arranged as following. Section II discusses about the formalism of how we model the 2-f to 3-f combustion and what is the velocity of combustion front. Section III discussed about the calculation and results of the GW signals and the general template of such PT. Finally, in Section IV we discuss our results and conclude from them.

2. 2-f to 3-f conversion

The shock induced combustion in NS is a two-step process. Due to sudden fluctuation at the center of the star a shock wave is generated at the core and propagates outwards first converting NM to 2-f QM. The initiation of such process can be anything which involves any density fluctuation at the center of the star. This can be star settling into an stable configuration during mass accretion or a pulsar glitch. The shock induced PT is also likely to occur in BNSM after the first merging during the hypermassive star stage. This conversion is a fast process and it has been previously shown that the speed of such shock front is close the speed of light Prasad & Mallick (2018, 2019). The outcome of the aftermath of such shock combustion the matter at the core of the star is unstable QM. The second step combustion is the conversion of 2-f QM to 3-f QM as 3-f QM is more stable at such high densities.

The conversion of 2-f to 3-f matter proceeds as a slow combustion where weak interaction governs the combustion process. The core of the star which have 2-f matter is unstable, and for stability it converts to 3-f matter. This happens via conversion of excess down quarks to strange quarks. Once beta equilibrium is attained for that particular radial point, the combustion front proceeds forward. The NM to QM conversion happens till the point where NM is more stable than QM. This point can be found by plotting the μ_b vs p curve for given choices of EoS governing

the NM and QM. Fig 1 shows the PT point. The crossing point of NM and 3-f matter is the PT point and for a given value of p the matter which has lower μ_b is more stable. Once this point is identified, solving the TOV equation gives the corresponding radial point inside the star. This is shown in fig 1.

We have used S271 (Lalazissis et al. 1997; Horowitz & Piekarewicz 2002) parameter setting to describe the NM and MIT bag model having quark interaction (Chodos et al. 1974; Alford et al. 2007; Weissenborn et al. 2011) for QM. Both the EoS are consistent with the recent nuclear and astrophysical constraints. For the QM the 2-f matter has only up and down quarks with masses 5 MeV, whereas 3-f matter also has strange quarks with mass 100 MeV. The bag constant is assumed to be $B^{1/4} = 140$ MeV and the strength of quark coupling is $a_4 = 0.5$.

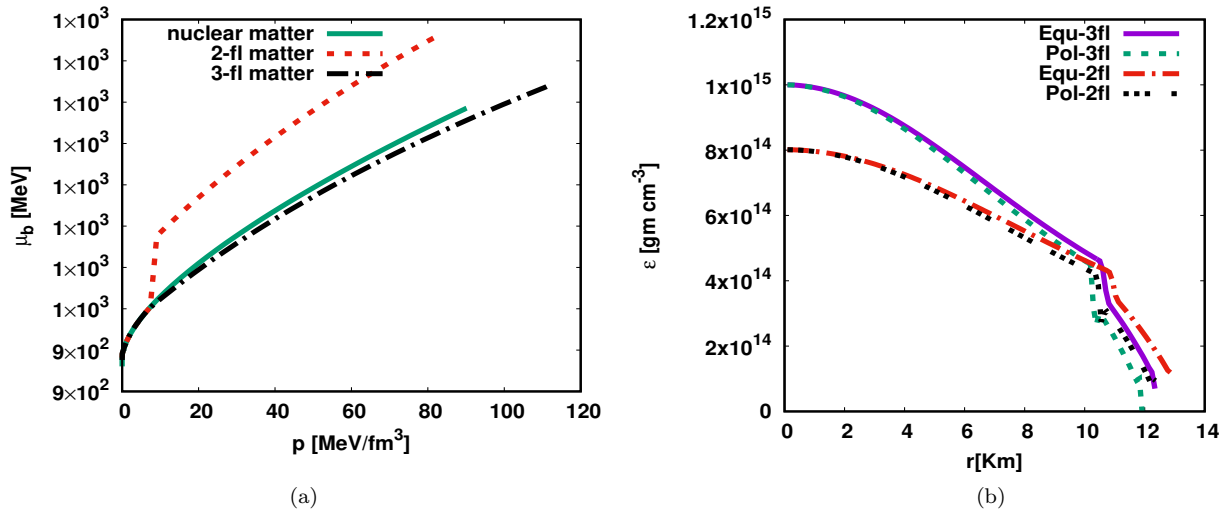


Fig. 1.— a) The μ_b against p curve for NM, 2-f QM, and 3-f QM is shown. The 3-f QM is more stable than NM at high densities. Although, NM is more stable than 2-f matter even at high densities, however, deconfinement would first happen and then it deconfined 2-f matter would settle into 3-f matter eventually. b) Energy density profile for both 2-fl and 3-fl matter in the equatorial and polar direction

For the generation of GW, the star in which PT happening should be axis-symmetric. This can happen for a rotating star. In our calculation we have used Hartle's slow rotation approach for constructing rotating star model (Hartle 1968; Hartle & Thorne 1968). This approach is quite accurate for stars whose rotational speed is few hundreds of Hz. In our calculation we have constructed stars with rotational speed of 50 and 500 Hz.

As we have a rotating star, the shape of the star is oblate spheroid. Therefore, the corresponding PT point along the equatorial and polar direction differs. One should mention that in a realistic scenario the NM to 2-f matter conversion may cross this point and proceed outwards, however, as the NM is more stable than 3-f matter beyond this radial point it will again convert back to NM. As the NM to 2-f matter scenario is discussed in detail previously (Prasad & Mallick

(2018, 2019)), we only discuss the 2-f to 3-f conversion in the present article.

The beta equilibrated 3-f matter is charge neutral and the baryon conservation still holds. This can be written as,

$$2n_u = n_d + n_s + 3n_{e^-} \quad (1)$$

$$3n_b = n_d + n_s + n_u \quad (2)$$

where n_b , n_u , n_d , n_s and n_{e^-} are baryon, up quark, down quark, strange quark and electron number densities respectively. Neglecting the interaction of matter and in the small temperature limit we can write the number density of species i in terms of chemical potential μ_i ($\frac{\mu_i}{T} \gg 1$).

$$n_i = \begin{cases} \frac{\mu_i^3}{\pi^2} & \text{for massless particles} \\ \frac{(\mu_i^2 - m_i^2)^{\frac{3}{2}}}{\pi^2} & \text{for particle having mass } m_i \end{cases} \quad (3)$$

We consider a frame of reference in which conversion front is stationary. It is also assumed that the volume in which conversion takes place to be much smaller than the total quark matter region. Therefore, the problem can be treated in one dimension. The density fluctuation deconfines the nuclear matter at the core of the star. Once the shock wave has propagated out, we have 2-f QM at the star core and the NM near the surface. The quark-nuclear transition point depends on the EoS, and for our choice of it is around 10 km. The unstable 2-f core has a excess of down quarks, which convert into the strange quarks via weak decay as long as $\mu_d > \mu_s$, given by

$$d \rightarrow u + e^- + \nu_{e^-}, \quad (4)$$

$$s \rightarrow u + e^- + \nu_{e^-}, \quad (5)$$

$$d + u \rightarrow s + u. \quad (6)$$

The conversion stops when $\mu_d = \mu_s$ and we have stable 3-f quark matter. At equilibrium, the chemical potential of the down and strange quark can be written in terms of chemical potential of up quark and electron assuming that neutrinos will escape freely from the star Bhattacharyya et al. (2006). Therefore, we have

$$\mu_d = \mu_s = \mu_u + \mu_{e^-}. \quad (7)$$

The conversion process starts at the center of the star and goes towards the surface in the region which is filled with the unstable 2-f matter.

To parametrize the PT, we define a quantity ‘ a ’ as function of radial co-ordinate r taking center of star as the origin,

$$a(r) = \frac{n_d(r) - n_s(r)}{2n_b(r)}, \quad (8)$$

such that at the center of star $a(r = 0) = a_0$, which is the minimum value of a for which strange matter is stable. For stable nuclear matter we have the condition $a(r = r_{nuc}) = 1$, where

r_{nuc} denotes the point where NM is stable. This can be understood from our definition of $a(r)$, where $n_s = 0$. The minimum value of $a(r)$ is zero where $n_d = n_s$, and which happens at asymptotically high density. From the above arguments it is clear that a_0 can take values from 0 to 1. However, for practical purpose it never goes to zero at the star center.

The conversion process can be studied through two process: first is decay of down quark into strange quark via weak decay (eqn 6), and the second diffusion of strange quark into matter. Defining $n_b R$ as the decay rate, the weak decay can be mathematically written as (Olinto 1991)

$$\begin{aligned} n_b R &= -\frac{dn_{dn}}{dt} = \frac{dn_{sg}}{dt}, \\ \Rightarrow 2n_b R &= -\frac{d(n_{dn} - n_{sg})}{dt}, \\ \Rightarrow R &= -\frac{d}{dt} \left(\frac{n_{dn} - n_{sg}}{2n_b} \right), \end{aligned}$$

which finally gives

$$\frac{da}{dt} = -R(a). \quad (9)$$

the weak decay equation.

The equation for diffusion of strange quark is given by

$$\frac{da}{dt} = D \frac{d^2 a}{dr^2}. \quad (10)$$

where D is diffusion coefficient (Bhattacharyya et al. 2006; Olinto 1991). D is expressed as

$$D \propto \left(\frac{\mu_b}{T} \right)^2 \quad \text{or} \quad D \simeq 10^{-3} \left(\frac{\mu_b}{T} \right)^2 \text{cm}^2 \text{s}^{-1}. \quad (11)$$

with the baryon chemical potential μ_b and temperature T are in MeV. Therefore, the change in a with time is given by (using 9 and 10)

$$\frac{da}{dt} = D \frac{d^2 a}{dr^2} - R(a). \quad (12)$$

From the usual definition of total derivative, we have

$$\frac{da}{dt} = \frac{\partial a}{\partial t} + (\vec{v} \cdot \vec{\nabla} a), \quad (13)$$

and for one dimensional steady flow $\frac{\partial a}{\partial t} = 0$, then this reduces to

$$\frac{da}{dt} = v \frac{da}{dr}. \quad (14)$$

Therefore, using eqn 12 and 14, we finally have

$$D \frac{d^2 a}{dr^2} - v \frac{da}{dr} - R(a) = 0.$$

This can be simply denoted by

$$Da'' - va' - R(a) = 0 \quad \text{where} \quad a'' \equiv \frac{d^2a}{dr^2}; \quad a' \equiv \frac{da}{dr}. \quad (15)$$

The Boundary Conditions

From our definition, at $r = 0$, we have

$$a(0) = a_0. \quad (16)$$

Let us assume that at conversion front is at a distance $r = \bar{r}$ from the center. In the rest frame of the front, the 2-f matter will come from right get converted into 3-f matter and goes towards left. We write the equation of conservation of flux current at \bar{r} as

$$n_{3f}v_{3f} = n_{2f}v_{2f}.$$

Eqn 15 can be integrated over small volume of cylinder whose axis coincides with r to give

$$\int_V a'' dV - \int_V va' dV - \int_V R(a) dV = 0.$$

Now assuming length of cylinder is 2ϵ and $\epsilon \rightarrow 0$, the above equation can be written as

$$\lim_{\epsilon \rightarrow 0} \int_{\bar{r}-\epsilon}^{\bar{r}+\epsilon} Da'' dr - \lim_{\epsilon \rightarrow 0} \int_{\bar{r}-\epsilon}^{\bar{r}+\epsilon} va' dr - \lim_{\epsilon \rightarrow 0} \int_{\bar{r}-\epsilon}^{\bar{r}+\epsilon} R(a) dr = 0.$$

In the limit of vanishing ϵ the third term in the above equation goes to zero. The first two can becomes

$$\lim_{\epsilon \rightarrow 0} \left\{ Da' \Big|_{\bar{r}-\epsilon}^{\bar{r}+\epsilon} - va \Big|_{\bar{r}-\epsilon}^{\bar{r}+\epsilon} \right\} = 0.$$

This is explicitly written as

$$D \lim_{\epsilon \rightarrow 0} [a'(\bar{r} + \epsilon) - a'(\bar{r} - \epsilon)] - v \lim_{\epsilon \rightarrow 0} [a(\bar{r} + \epsilon) - a(\bar{r} - \epsilon)] = 0,$$

or

$$D[a'|_r - a'|_l] = v[a|_r - a|_l].$$

From our choice of reference frame, the right hand side has only 2-f matter, therefore, we have

$$a|_r = 1,$$

and

$$a'|_r = 0.$$

In the left hand side there is 3-fl matter then $a'|_l = a'(r')$. With the same argument at $r' = 0 = r$, we have

$$a'(0) = -\frac{v}{D}(1 - a_0). \quad (17)$$

Coming back to the main differential equation, in the low temperature limit we can write the decay rate $R(a)$ as given by (Olinto 1991).

$$R(a) \simeq \frac{16}{15\pi^3} G_F^2 \cos^2 \theta_c \sin^2 \theta_c \mu_{up}^5 \left(\frac{a^3}{3} \right) = \frac{a^3}{\tau}. \quad (18)$$

where

$$\tau = 1.399 \times 10^{-20} \mu_u^5. \quad (19)$$

Redefining x as $x = \eta \xi$ and $\eta = \frac{D}{v}$, DE 15 is written as

$$\frac{d^2 a}{d\xi^2} - \frac{da}{d\xi} - g a^3 = 0. \quad (20)$$

where

$$g \equiv \frac{D}{\tau v^2}. \quad (21)$$

The BC (17) then takes the form

$$\frac{da}{d\xi}(0) \equiv \frac{da}{d\xi} \Big|_0 = -(1 - a_0). \quad (22)$$

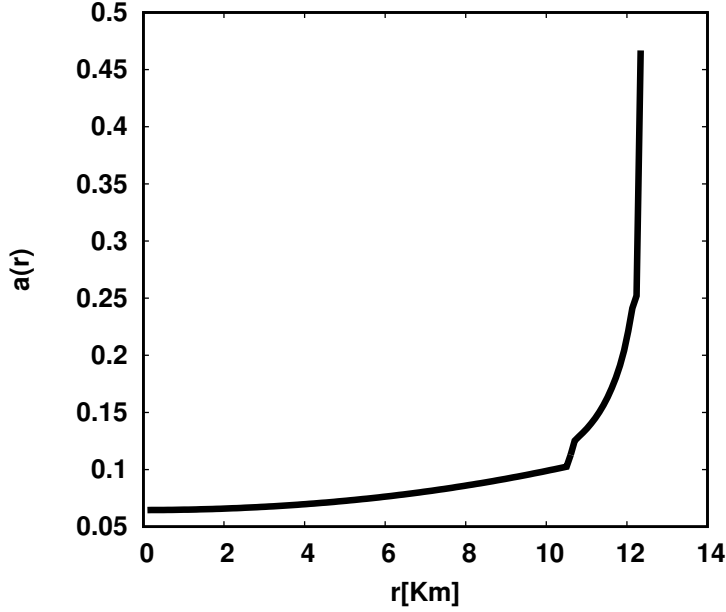


Fig. 2.— ratio $a(r)$ inside star at a distance r from the center of the star.

The DE 20 can be solved numerically using BC 16 and 22 for a given value of a_0 and g . We assume initially that there is a 3-f equilibrated seed at the star center. This fixes the value of a_0 for our condition. We solved TOV eqn for slowly rotating star to get density as the function of

r of quark star (fig 1). In the process of conversion the baryonic mass M_b remains constant. In fig 1 we have plotted energy density vs radius for both along the equatorial and polar direction. For the Baryonic mass of the star $M_b = 2.08678M_\odot$, the gravitational mass of 2-f and 3-f stars are $M_{2f} = 1.8475M_\odot$ and $M_{3f} = 1.8416M_\odot$ respectively.

After finding number density we can find a at any radial point, and is shown in fig 2. The value of a is minimum at the center, which is a_0 . As we proceed outward of the star a increases and it is maximum at the point where the PT stops and NM is stable. The maximum value of a for which 3fl matter is stable will be at the center of star which is $a_0 = 0.06457671$.

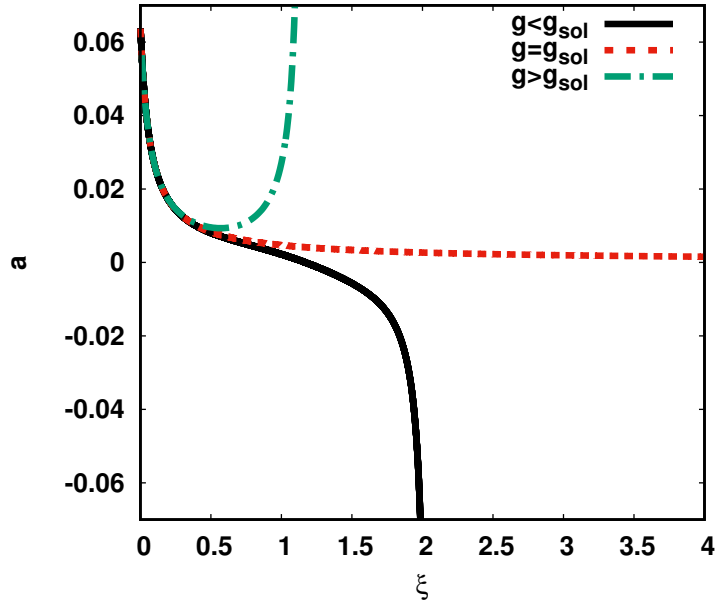


Fig. 3.— Numerical solution of d.e.20 taking initially $a_0 = 6.457671 \times 10^{-2}$. In this graph we have plotted a vs ξ for three different values of g : $g = 105210 < g_s$, $g = 105215.786249 = g_s$ and $g = 105220 > g_s$; here g_s correspond to value of g for which solution is valid.

Next task is to calculate the value of g . To solve the differential equation we need to know g . However, initially g is g unknown. Therefore, what we do is to start with some value of g and then solve the differential equation. To get an unique solution of the DE we must know the nature of a in the star. As we discuss earlier that a can take value between 0 and 1 which is always positive. Therefore, $\frac{da}{d\xi}$ will be negative (from eqn 22), and therefore a is a monotonically decreasing function. For given a_0 , we solve eqn 20 for different value of g , however, only one of g gives the correct solution g_s . If $g < g_s$ then solution of DE undershoots and if $g > g_s$ then solution overshoots (see fig 3 (a)). By narrow downing these value of g we find g_s . After finding g_s we can find conversion velocity v from the eqn 21 and is given by

$$v = \sqrt{\frac{D}{\tau g_s}}. \quad (23)$$

With a given value of a_0 , we solve DE 20 to find g as described above and shown in fig 3 (a). We start with a given value of g and solve the DE and by trial and error method we find the given solution of g within error estimates. Once we find g_s we then can calculate the velocity of the front. The value of g_s for our case comes out to be $g = 105215.786249$.

To find the velocity, one needs to find the number densities of various species in the star. To do that we make use of the assumption that with no mass loss during the conversion process, and therefore baryon number conservation and charge neutrality still holds (eqns 2). Using the density profile and using eqns 2, 3 and 7 we can find number density of various species inside the star as function of r . In our calculation we assume up and down quark are massless but strange quark has mass $m_s \approx 100 MeV$. The equations for finding the number density are as follows

$$n_u = n_b + n_{e^-}. \quad (24)$$

$$n_{e^-} = \frac{\mu_{e^-}^3}{\pi^2}. \quad (25)$$

$$n_d = \frac{((n_s \pi^2)^{\frac{2}{3}} + m_s^2)}{\pi^2}. \quad (26)$$

$$n_s + \frac{[(n_s \pi^2)^{\frac{2}{3}} - m_s^2]^{\frac{3}{2}}}{\pi^2} + n_{e^-} = 2 n_b. \quad (27)$$

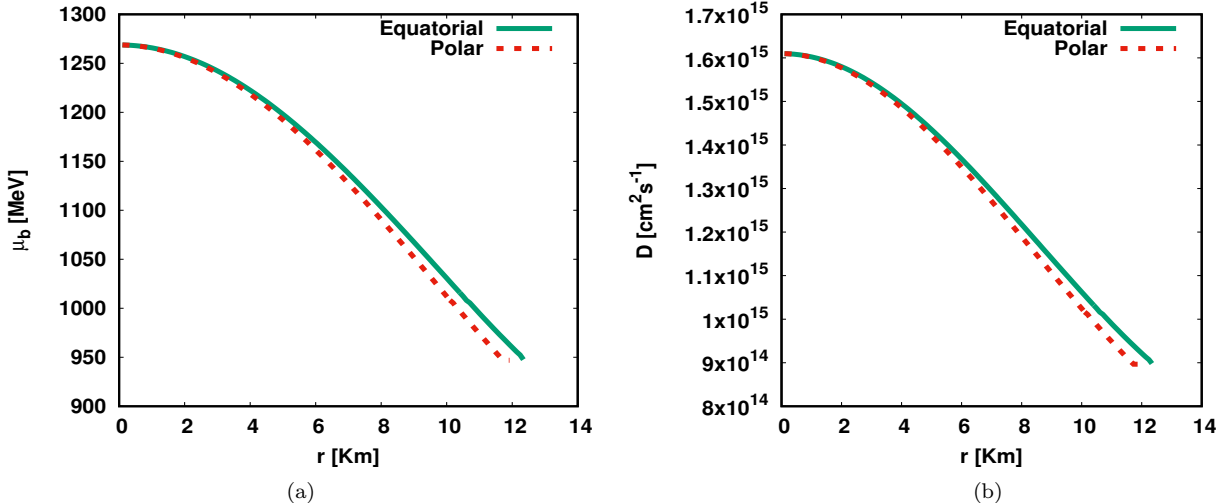


Fig. 4.— a) Baryonic chemical potential μ_b as function of r in side the star in equatorial and polar direction. b) Diffusion coefficient D as function of r in side the star in equatorial and polar direction

To find the velocity along with g_s two other quantities are also needed to be calculated, D and τ . As is shown in eqn 11, D is a function of μ_b , and from the star profile we find μ_b as a function of r . Therefore, we can get D as a function of r . The variation of μ_b as a function of r is shown

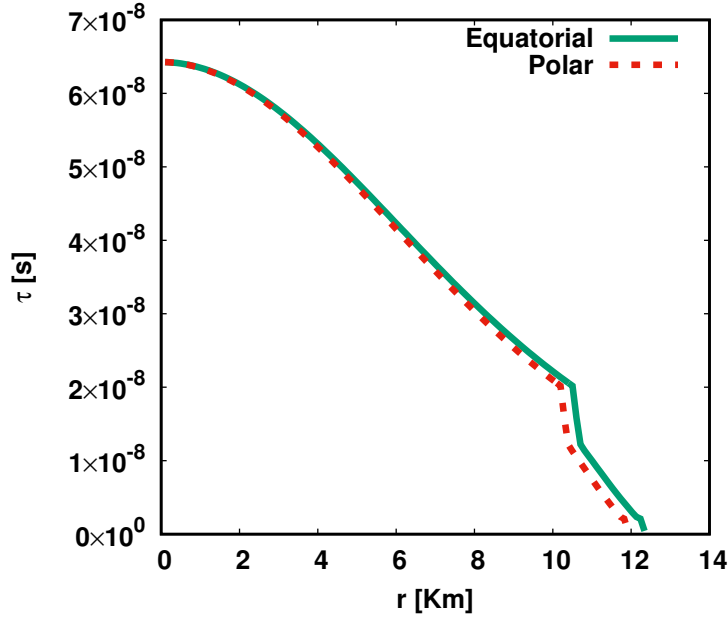


Fig. 5.— ratio $a(r)$ inside star at a distance r from the center of the star.

in fig 4 (a). As expected the chemical potential falls off as we go outwards of the star. The fall is smooth and monotonic till the point where PT stops. Beyond the PT point, the fall in μ_b is fast and gets saturated around 950 MeV. D also depends on the star temperature and for a cold NS we assume that the temperature of the star is constant throughout and assumed its value to be equal to 10^{-6} MeV. Therefore, with this assumption D directly depends on μ_b the behavior of D closely resembles that of μ_b as shown in fig 4 (b). It starts with a high central value at the star center and falls off as we proceed outwards. Again, there is a discontinuity at the PT point inside the star. The final parameter that remains to be calculate is τ . The value of τ is directly proportional to μ_u^5 , as given in eqn 19. Knowing the number density of up quark, the chemical potential of the up quark is calculated from eqn 3. The up chemical potential also depends on the radial distance from the star center. Calculating the up chemical potential, the variation of τ as a function of radial distance is shown in fig 5.

Finally in figure 6 (a) we plot how the velocity of the conversion front varies with distance from the star center. The value of v at the star center is about $0.00163c$ and initially as we move towards the surface of the star it monotonically increases up to PT point after that it shoots up to a value $0.1c$. However, the variation of the velocity with radial distance is not huge till PT point. After knowing the velocity profile we can find position of conversion front and total conversion time by integrating eqn $dt = \frac{dr}{v(r)}$. The total conversion time found to be 1.96×10^{-3} s.

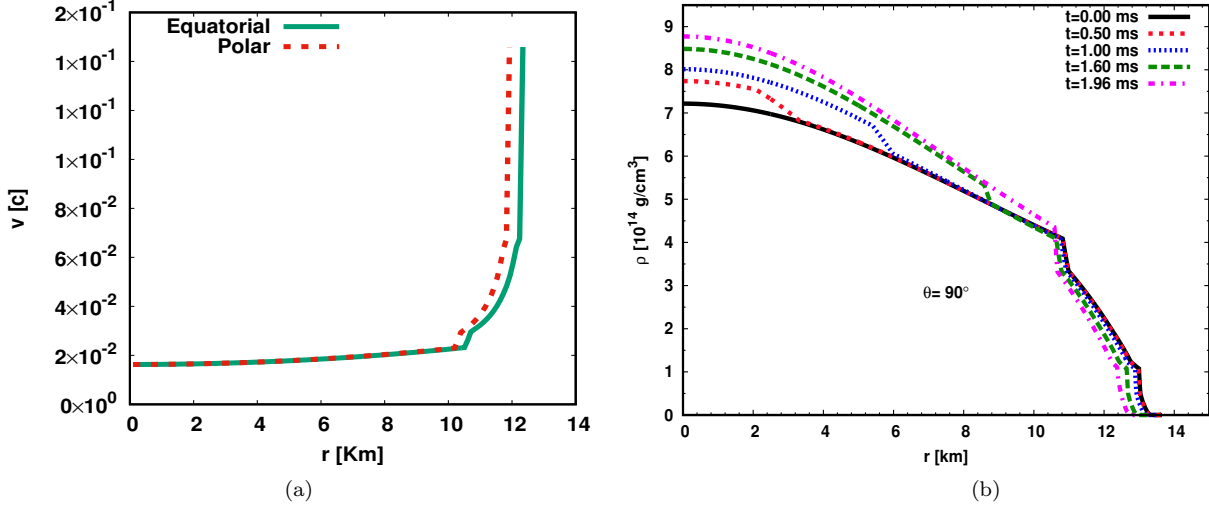


Fig. 6.— a) Conversion velocity inside star at a distance r from the center of the star in equatorial and polar direction. b) Conversion front inside the star at various time.

3. Gravitational waves

Solving the TOV, and with our construction we find a_0 , g_s and the front velocity inside the star. From our assumption the conversion front starts from the star center and moves outwards. In the process it converts 2-f matter to 3-f matter, where the front velocity is governed by the weak decay rate and diffusion coefficient. As the front velocity depends on the radial position, we can find the front position at any given time from eqn $v(r) = \frac{dr}{dt}$. Let us say at a time t' the front has reached at a radius r' , then in the region $r < r'$ there will be 3-fl matter and for $r > r'$ 2fl there will be matter. This helps us calculating the change in the density profile of the star as the front moves from the star to the surface. The change in density profile as a function of time is shown in figure 6 (b). The density profile are shown for four time sequences. Once the change in density profile as a function of time is known we proceed to find the gravitational wave amplitude as done previously in our earlier paper Prasad & Mallick (2019).

The non-zero components of the wave amplitude for an axis-symmetric star is given by (Zwerger 1997; Dimmelheimer et al. 2002)

$$h_{\theta\theta}^{TT} = \frac{1}{8} \sqrt{\frac{15}{\pi}} \sin^2 \theta \frac{A_{20}^{E2}}{r}, \quad (28)$$

$$h_{\phi\phi}^{TT} = -h_{\theta\theta}^{TT} = h_+ \quad (29)$$

where θ is the misalignment angle between the stars symmetry axis and the observer line of view. A_{20}^{E2} is given by

$$A_{20}^{E2} = \frac{d^2}{dt^2} \left(k \int \rho \left(\frac{3}{2} z^2 - \frac{1}{2} \right) r^4 dr dz \right) \quad (30)$$

with $z = \cos \theta$ and $k = \frac{16\pi^{3/2}}{\sqrt{15}}$.

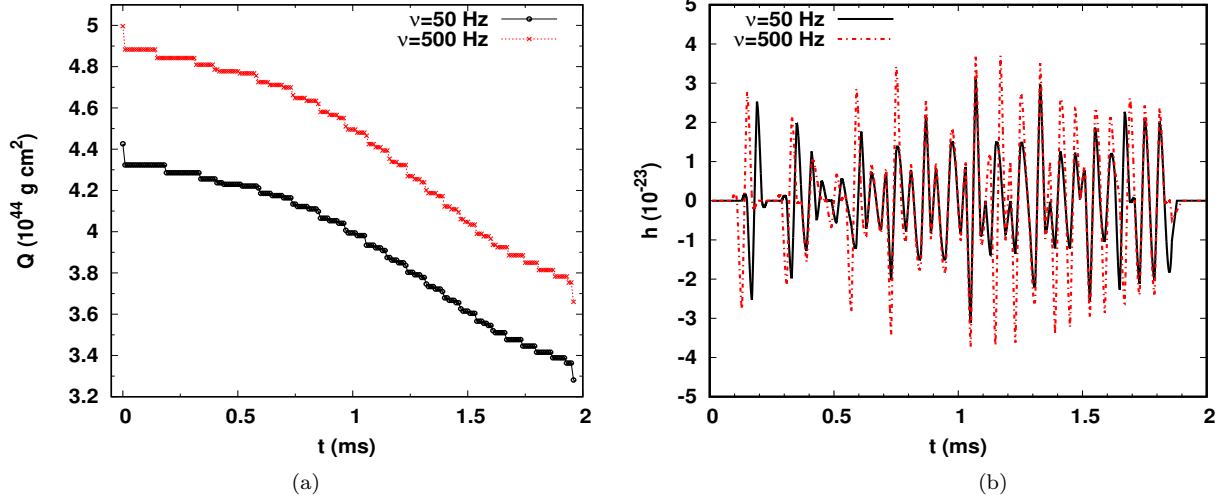


Fig. 7.— a) The change in quadrupole moment as a function of time is shown b) The GW amplitude is illustrated for the conversion of 2-f to 3-f matter in HS. The duration of the signal is 1.96 ms.

We assume that at time $t = 0$, the 3-f seed originate at the center of the star. Knowing the velocity we locate of the conversion front after a small time interval ($dt = 10^{-6}$ sec). Once we know this location we know that at this position the RHS has 2-f matter and LHS has 3-f matter. We get the density profile of the star, and integrating it we get the quadrupole moment. The steps are repeated till the PT point, and we obtain the quadrupole moment and the GW amplitude using the above equation.

In fig 7 (a) we plot the quadrupole moment as a function of time. The quadrupole change for both the stars (with $\Omega = 50 \text{ Hz}$ and 500 Hz) are shown in the plot. As the density profile of the star is rearranged at every time step, the quadrupole moment of the star changes. However, the quadrupole moment (QMoM) decreases globally with time for both the stars. The initial QMoM of the fast rotating star is higher than the slow star. The stars are assumed to be at located 10 Mpc. The change of QMoM with time is reflected in the GW amplitude of both the stars. This is shown in fig 7 (b). The GW amplitude is of the order of $10^{-24} - 10^{-23}$ for both the stars. Although the QMoM of the fast star is greater than that of the slow star the change in the QMoM with time is similar for both stars, therefore the GW strain is also similar for both the stars. This also means that the energy release from the PT of NS to QS conversion is very similar for both the stars and the rotation does not play a very significant role in determining the nature of GW.

The corresponding power spectra is obtained by moving to the corresponding Fourier space of the time domain signal of $h(t)$ with $0 \leq t \leq T$, and is given by (Press et al. 1992; Dimmelheimer et al. 2002),

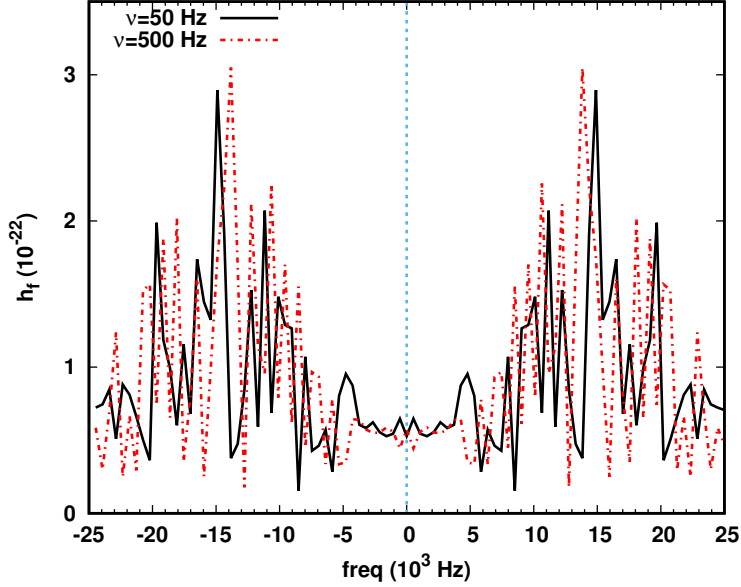


Fig. 8.— The power spectrum of the GW signal for 2-f to 3-f phase transition. The power has a significant peaks in 15 – 20 KHz.

$$\tilde{h}_k = \sum_{n=0}^{N-1} h_n \exp \left(\frac{2\pi i n k}{N} \right) \quad (31)$$

with the corresponding frequency

$$\omega = \frac{2\pi k}{T}.$$

The power spectrum is expressed as,

$$P(\omega) = \frac{|\tilde{h}_k|^2}{N^2}. \quad (32)$$

Maintaining the common procedure the amplitude spectrum $h(\omega) = \sqrt{P(\omega)}$ is plotted as function of frequency $f = \frac{\omega}{2\pi}$.

In fig 8 we plot the power spectrum of the GW for both the stars. The signal from $t = 0$ to $t = 1.87$ ms is sampled with a sampling time of $\Delta t = 2 \times 10^{-5}$ s, and then the discrete Fourier transform is performed. We find that for both the stars the peak frequencies are present around 10 – 20 KHz, implying that most of the power is accumulated there. The peak frequency is near about at the extreme end of present detectors, however, proposed detectors which are being constructed can easily detect such peak frequency.

Summary and Conclusion

In this work we have studied the PT of NM to stable 3-f quark matter and especially we have calculated the template of GW amplitude that can be emitted from the conversion the 2-f to 3-f matter at the star core. The weak conversion of 2-f matter to 3-f matter is calculated here which follows a shock induced deconfinement of NM to 2-f matter. The shock induced PT happens due to a sudden density fluctuation at the star core. The shock produces a deconfined seed of 2-f matter at a small region of the star core. As the EoS of 2-f QM is very different than that of NM, there is a sudden discontinuity in density at the star core. This density discontinuity gives rise to a shock wave at the core, which then propagates outwards with time. This shock is strong enough to combust NM to 2-f QM and mimics a PT in the star. The 2-f QM is not stable and there is an excess of d quarks. The 2-f matter settles to a stable 3-f matter in the weak time-scale Bhattacharyya et al. (2006); Olinto (1991); Niebergal et al. (2010).

To study this conversion of 2-f matter to 3-f matter involves decay of down quarks to strange quarks and also the diffusion of quarks across the front boundary. The diffusion rate and the weak reaction rate is calculated from the chemical potential of 3-f QM which varies across the star. Knowing this rates, we finally solve the DE of a to find the velocity of the conversion front. The conversion velocity is about 0.007 times of speed of light and the time taken for the conversion is about 6 millisecond. Once the front velocity is known we find the change in density profile of the star as a function of time as 2-f matter settles into 3-f QM.

As the conversion moves out, the density profile changes along with it. This gives rise to the change in the quadrupole moment. The change is maximum at the PB, where the conversion front stops. Thus we have an HS, with a stable 3-f quark core and NM outer layer. The energy released during such PT is emitted as GW signals and has an oscillating behavior when the conversion front stalls near the boundary and the energy is transmitted out. This change in QM is quite significant, and the GW amplitude comes out to be of the order 10^{-23} , which is also notable and can be detectable with present and next-generation GW detectors. The power spectrum of such a GW signal shows mostly a peak frequencies at about 15 – 20 kHz, which is on the higher side of detector capability, however, proposed detectors would soon cover such frequency range.

If such a GW amplitude and frequency can be detected, it would imply that NS do undergo PT at such densities and the PT is a strong first order. However, such a GW signal is possible if the conversion front stops at some distance inside the star. The radial position of PB depends strongly on the choices of the EoS, however, the PB is inevitable. We have performed this calculation in a cold NS, however, BNSM are more susceptible to such type of PT. Such PT signatures are also a unique feature of shock induced PT, where the combustion front follows a shock. However, a equilibrium PT does not produce such signals and then only indirect evidence of PT are the only way to deduce the PT in NSs.

The author RM is grateful to the SERB, Govt. of India for monetary support in the form

of Ramanujan Fellowship (SB/S2/RJN-061/2015). RP would like to acknowledge the financial support in the form of INSPIRE fellowship provided by DST, India. SS, RM and RP would also like to thank IISER Bhopal for providing all the research and infrastructure facilities.

REFERENCES

B. P. Abbott et al. (LIGO Scientific Collaboration and Virgo Collaboration), *Phys. Rev. Lett.* **119**, 161101 (2017)

E. B. Abdikamalov, H. Dimmelmeier, L. Rezzolla & J. C. Miller, *Mon. Not. R. Astron. Soc.* **392**, 52 (2009)

A. Bhattacharyya, S. K. Ghosh, P. S. Joarder, R. Mallick & S. Raha, *Phys. Rev. C* **74**, 065804 (2006)

A. R. Bodmer, *Phys. Rev. D* **4**, 1601 (1971)

A. Chodos, R. L. Jaffe, K. Johnson, C. B. Thorn & V. F. Weisskopf, *Phys. Rev. D* **9**, 3471 (1974)

Dimmelmeier H., Font J. A., Mueller E., *Astron. & Astrophys.* **393**, 523 (2002)

A. Ferrari and R. Ruffini, *Astrophys. J.* **158**, L71 (1969)

R. Mallick and M. Irfan, *MNRAS* **485**, 577 (2019)

E. R. Most, L. R. Weih, L. Rezzolla, and J. Schaffner-Bielich, *Phys. Rev. Lett.* **120**, 261103 (2018)

R. Prasad & R. Mallick, *Astrophys. J.* **859**, 57 (2018)

J. A. Faber and F. A. Rasio, *Living Rev. Relativity* **15**, 8 (2012)

L. Baiotti and L. Rezzolla, *Rep. Prog. Phys.* **80**, 096901 (2017)

T. Krger, I. Tews, K. Hebeler, and A. Schwenk, *Phys. Rev. C* **88**, 025802 (2013)

A. Bauswein, Niels-Uwe F. Bastian, D. B. Blaschke, K. Chatzioannou, J. A. Clark, T. Fischer, and M. Oertel, *Phys. Rev. Lett* **122**, 061102 (2019)

T. Hinderer, *Astrophys. J.* **677**, 1216 (2008)

J. S. Read, C. Markakis, M. Shibata, K. Ury, J. D. E. Creighton, and J. L. Friedman, *Phys. Rev. D* **79**, 124033 (2009)

W. Del Pozzo, T. G. F. Li, M. Agathos, C. Van Den Broeck, and S. Vitale, *Phys. Rev. Lett.* **111**, 071101 (2013)

M. Agathos, J. Meidam, W. Del Pozzo, T. G. F. Li, M. Tompitak, J. Veitch, S. Vitale, and C. Van Den Broeck, Phys. Rev. D 92, 023012 (2015)

K. Chatzioannou, C.-J. Haster, and A. Zimmerman, Phys. Rev. D 97, 104036 (2018)

A. Olinto, Phys. Lett. B 192, 71 (1987); Nucl. Phys. B 24, 103 (1991)

A. Drago, A. Lavagno and I. Parenti, Astrophys. J. 659 (2007) 1519

I. Mishustin, R. Mallick, R. Nandi, and L. Satarov, Phys. Rev. C 91, 055806 (2015)

R. Prasad, & R. Mallick, arXiv:1908.03889

Brian Niebergal, 1 Rachid Ouyed, 1 and Prashanth Jaikumar, Phys. Rev. C 82, 062801 (2010)

Zwerger, T. & Mueller, E., Astron. Astrophys., 320, 209 (1997)

G. A. Lalazissis, J. Konig, and P. Ring, Phys. Rev. C 55, 540 (1997)

C. J. Horowitz and J. Piekarewicz, Phys. Rev. C 66, 055803 (2002)

Press, W. H., Teukolsky, S. A., Vetterling, W. T., & Flannery, B. P. 1992, Numerical recipes in C: The art of scientific programming (Cambridge, U. K.: Cambridge University Press)

M. Alford, D. Blaschke, A. Drago et al., Nature (London) 445, E7 (2007)

S. Weissenborn, I. Sagert, G. Pagliara, M. Hempel, and J. Schaffner-Bielich, Astrophys. J. Lett. 740, L14 (2011)

J. B. Hartle, Astrophys. J. 150, 1005 (1967)

J. B. Hartle & K. S. Thorne , Astrophys. J. 153, 807 (1968)